JOURNAL OF MATERIALS SCIENCE 28 (1993) 611–620

Influence of heat treatment on the tensile properties and fracture behaviour of an aluminium alloy–ceramic particle composite

T. S. SRIVATSAN, J. MATTINGLY
Department of Mechanical Engineering, The University of Akron, Akron, OH 44325, USA

The tensile deformation and fracture behaviour of aluminium alloy 2124 reinforced with different amounts of silicon carbide particulates was studied, in the as-extruded and heat-treated conditions, with the objective of investigating the influence of heat treatment and composite microstructural effects on tensile properties and quasi-static fracture behaviour. Results indicate that for a given microstructural condition, the elastic modulus and strength of the metal-matrix composite increased with reinforcement content in the metal matrix. For a given volume fraction of reinforcement, the heat-treated composite exhibited significantly improved modulus and strength–ductility relationships over the as-extruded counterpart. The increased strength of the Al–SiC composite is attributed to the competing and synergistic influence of strengthening precipitates in the matrix metal, residual stresses generated due to intrinsic differences in thermal expansion coefficients between components of the composite and strengthening from constrained plastic flow and triaxiality in the ductile matrix due to the presence of brittle reinforcement. Fracture on a microscopic scale is initiated by cracking of the individual or clusters of SiC particles present in the microstructure. Particle cracking was dominant for the as-extruded composite microstructure. For both the as-extruded and heat-treated conditions, particle cracking increased with reinforcement content in the matrix. Final fracture of the composite resulted from crack propagation through the matrix between clusters. Although these composites exhibited limited ductility on a macroscopic scale, on a microscopic scale the fracture mechanism revealed features reminiscent of ductile failure.

1. Introduction

The emergence of novel processing techniques coupled with the need for lighter materials with high specific strengths and stiffnesses has catalyzed considerable scientific and technological interest in the development of numerous high-performance composite or hybrid materials as serious competitors to the traditional engineering alloys. The majority of such materials are metallic matrices reinforced with high-strength, high-modulus and often brittle second phases, in the form of fibres, whiskers or particulates, embedded in a ductile metal matrix. The reinforced metal matrices offer potential for significant improvements in efficiency, reliability and mechanical performance over the traditional and newer generation monolithic alloys.

Reinforced metal-matrix composites (MMCs) offer advantages in applications where low density, high strength and high stiffness are of primary concern. The aligned continuous fibre-reinforced composites offer very high directional properties such as high specific stiffness along the reinforcement direction [1]. Conversely, in applications where such extreme properties are not a requirement, the discontinuous metal-matrix composites consisting of particulates, whiskers or nodules are preferred, because they offer substantially improved strength and modulus properties compared to the monolithic alloy and provide the additional advantage of being machinable and workable. In particular, the particulate-reinforced metal-matrix composites are attractive because they exhibit near isotropic properties when compared to the continuously reinforced counterparts, and are easier to process using standard metallurgical processing such as powder metallurgy, direct casting, rolling and extrusion. The primary disadvantage of all MMCs, however, is that they suffer from low ductility, inadequate fracture toughness and inferior fatigue crack growth performance compared to that of the constituent matrix material [2–8]. A large body of published literature covering both theoretical and experimental aspects is available on the mechanical behaviour of metal-matrix composites [9–39].

The addition of silicon carbide particles to aluminium alloys results in an increased elastic modulus, due to the higher elastic modulus of the silicon carbide (SiC), which may also be accompanied by an increased flow stress, depending on the matrix alloy chosen, heat treatment and manufacturing method used [40]. Other significant advantages of discontinuously reinforced aluminium alloy metal-matrix composites are enhanced resistance to wear [41], corrosion [42] and

0022–2461

fatigue crack initiation resistance [43] when compared to the matrix material.

The present study was undertaken with the objective of evaluating the influence of heat treatment on the tensile properties and fracture behaviour of SiC particulate-reinforced aluminium alloy metal-matrix composite. In the experimental programme an evaluation of tensile properties and fracture behaviour was carried out for different volume fractions of ceramic particle reinforcement in the aluminium alloy matrix. The properties of the heat-treated composite material are compared with those in the as-extruded condition in order to rationalize composite microstructural influences on tensile properties and fracture behaviour.

2. Material

The material used in this experimental investigation was a powder metallurgy aluminium alloy (2124) reinforced with varying volume fractions of silicon carbide particulates (SiC_p). Three different volume fractions (20, 25 and 30 vol%) of SiC_p were chosen. The chemical composition (in weight per cent) of the matrix alloy is listed in Table I. The material was donated by DWA Composite Specialties Inc. Chatsworth, CA and is manufactured using standard powder metallurgy techniques. The silicon carbide particulates were mechanically mixed with the aluminium alloy powder, which is then hot compacted and subsequently extruded to bars of length 350 mm and having a rectangular cross-section approximately 95 mm (b) × 35 mm (t). Extrusion ratios are unknown. The metal-matrix composites were received in the as-extruded and heat-treated (T4) condition. The heat treatment consisted of solution treating the as-extruded MMCs at 920 °F (498 °C) for 2 h, water quenching and subsequently precipitation ageing at 250 °F (120 °C) for 18 h to give the T4 temper. In order to establish a basis for the comparison of the mechanical behaviour of the composite, the matrix alloy (synthesized from the same powder batch) with no SiC reinforcement and with an identical processing history and heat treatment (T4) was also studied.

The initial microstructure of the as-received material was characterized by optical microscopy after standard metallographic preparation techniques.

TABLE I Chemical composition (wt %) of matrix alloy 2124

Cu	Mg	Zn	Mn	Si	Fe	Ti	Al
4.65	1.65	0.01	0.9	0.04	0.30	–	Bal.

3. Experimental procedure

Tensile test specimens were machined such that the longitudinal direction or major stress axis of each specimen was parallel to the extrusion direction of the as-received plate. Thus, the gross fracture plane was perpendicular to the extrusion direction in each case. The cyclindrical tensile specimens conformed to standards specified in ASTM E-8, with threaded ends and a gauge length which measured 26 mm long and 6.25 mm diameter. To minimize the effects of surface irregularities and finish, the gauge sections were ground, using 600 grit silicon carbide paper, in order to remove all circumferential scratches and machine marks. Uniaxial tensile tests were performed on a computer-controlled servohydraulic test machine in

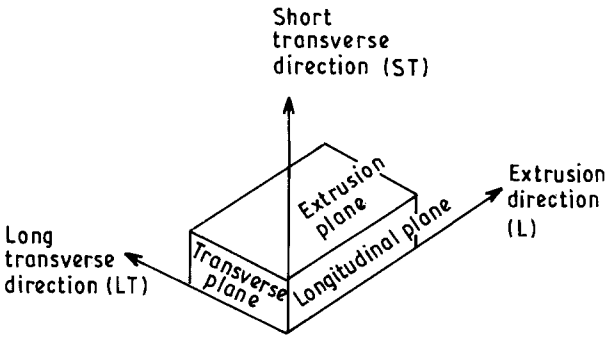

Figure 1 Triplanar optical micrographs illustrating the microstructure of the as-extruded 2124 composite with (a) 20 vol% SiC_p, and (b) 30 vol% SiC_p.

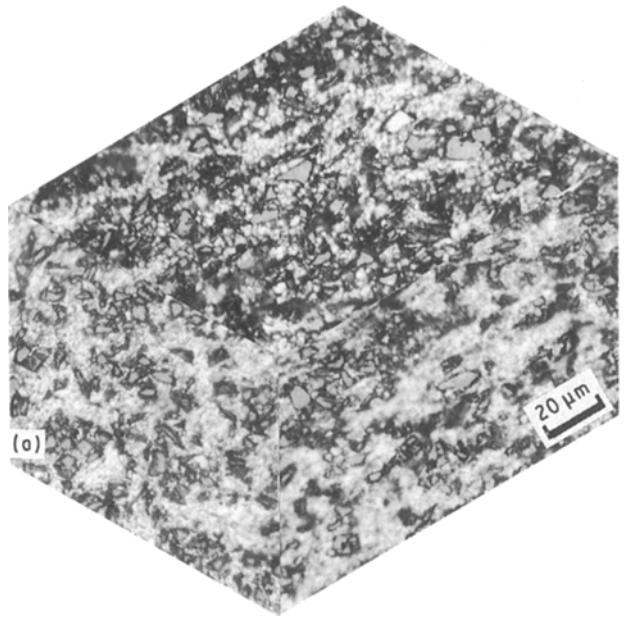

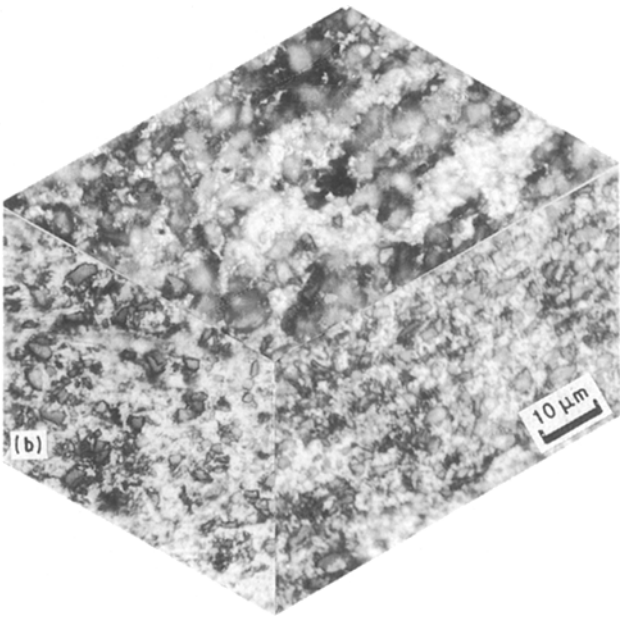

the room temperature (300 K) environment. Composite specimens were deformed at a constant strain rate of $10^{-4}\,s^{-1}$. The load and displacements parallel to the load line were recorded.

Fracture surfaces of the deformed tensile specimens were examined in a scanning electron microscope in order to characterize the fracture mode and the fine-scale features on the fracture surface.

4. Results and discussion

4.1. Initial microstructure

The triplanar optical micrographs illustrating the grain structure of the as-extruded, and heat-treated and aged composites, for different volume fractions of SiC reinforcement, are shown in Figs 1 and 2. For the as-extruded material, the discontinuous SiC particulates were found dispersed randomly through the matrix of the aluminium alloy. At regular intervals clustering or agglomeration of SiC particulates was found. The non-uniform distribution of particulates along the three orthogonal directions (extrusion, long-transverse and short transverse) of the as-extruded plate results in an anisotropic microstructure of the composite.

The microstructure of the heat-treated composite is shown in Fig. 2. Heat treatment of the as-extruded composite was found to have no influence on particulate size, agglomeration and distribution. Agglomeration of silicon carbide particulates was evident along all three directions of the as-received plate. The matrix of the heat-treated composite consisted of very fine grains which could not be clearly resolved in the optical microscope.

4.2. Tensile properties

The ambient temperature tensile properties of the aluminium alloy metal-matrix composite (2124

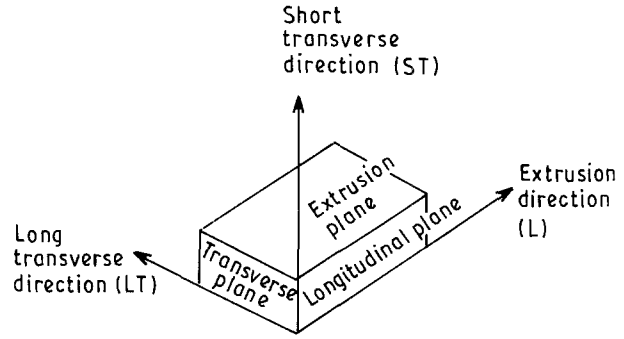

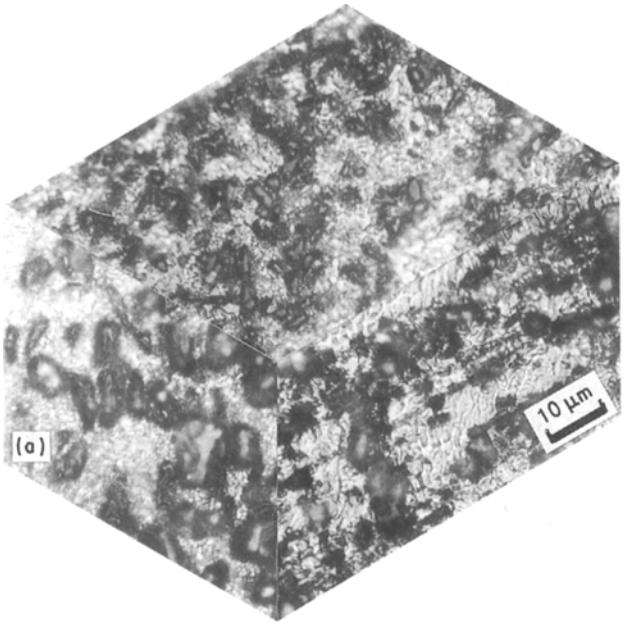

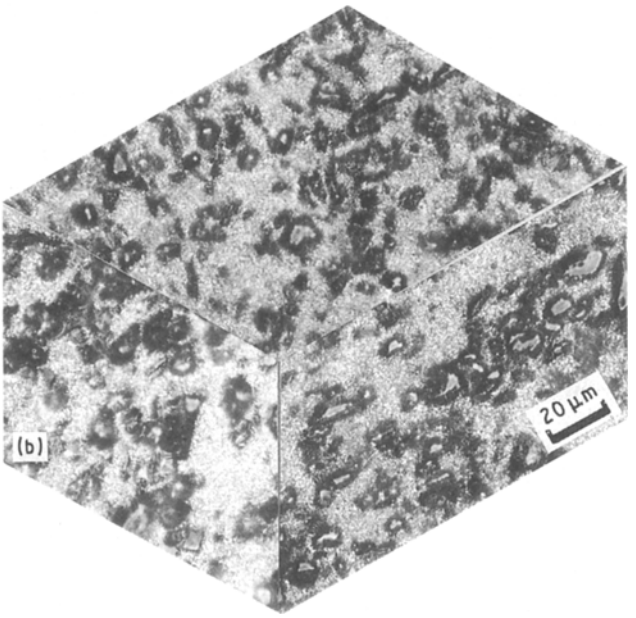

Figure 2 Triplanar optical micrographs illustrating the microstructure of the heat-treated 2124 aluminium alloy composites with (a) 20 vol% SiC_p, and (b) 30 vol% SiC_p.

TABLE II Monotonic mechanical properties[a] of 2124 Al–SiC composite, F-temper

Silicon carbide content (%)	E[b] (GPa)	Yield strength (MPa)	Ultimate tensile strength (MPa)	Elongation (%)	Reduction in area (%)	Fracture stress (MPa)
20	87	198	312	6.2	6.5	332
25	102	199	337	7.8	5.8	356
30	109	217	352	3.8	4.1	390

[a] Results are mean based on two tests
[b] Tangency measurements based on extensometer trace.

TABLE III Monotonic mechanical properties[a] of 2124 aluminium alloy, T-4 temper

Silicon carbide content (%)	Modulus of elasticity[b] (GPa)	Yield strength (MPa)	Ultimate tensile strength (MPa)	Elongation (G.L. = 1 in) (%)	Reduction in area (%)	True fracture stress (MPa)	n	K (MPa)
0	71	327	491	18	17.5	535	0.13	625
20	95	351	537	10.5	12.4	603	0.17	874
25	108	360	545	8.5	10.2	600	0.15	863
30	114	387	543	5.2	7.84	586	0.15	847

[a] Results are mean based on two tests
[b] Tangency measurements based on extensometer trace.

+ SiC_p), for different volume fractions of ceramic particle reinforcement, are summarized in Table II for the as-extruded composite and Table III for the heat-treated (T4) composite. The results are the mean values based on duplicate tests.

4.2.1. Elastic modulus

Tensile test results reveal, for a given microstructural condition, an increase in elastic modulus (Fig. 3) with an increase in SiC_p content in the aluminium alloy matrix. For the as-extruded composite microstructure the elastic modulus of the matrix alloy (2124) with 30 vol% SiC is 109 GPa which is:

(i) 25% more than the elastic modulus of the matrix alloy with 20 vol% SiC reinforcement (87 GPa), and
(ii) 55% more than that of the alloy with no SiC_p reinforcement (0 vol%) (69 GPa), that is, the unreinforced matrix.

For the heat-treated composite the elastic modulus of the matrix material with 30 vol% reinforcement is 114 GPa, which is:

(i) 20% more than the elastic modulus of the matrix having 20 vol% reinforcement (95 GPa), and
(ii) 61% more than that of the alloy with no reinforcement (0 vol%) (71 GPa).

Furthermore, for a given volume fraction of reinforcement, heat treatment of the aluminium alloy metal-matrix composite was observed to have a marginal influence on the elastic modulus of the composite. The improvement was as high as 15% for the composite with 30 vol% reinforcement.

4.2.2. Strength

The increase in yield strength (which is defined as the stress required at a plastic strain of 0.2%) due to the addition of SiC reinforcement was only marginal for the as-extruded composites. The matrix alloy with 30 vol% SiC had a 10% higher yield strength (217 MPa) than the aluminium alloy matrix with 20 vol% SiC reinforcement (198 MPa). A similar improvement in yield strength was noticed for the heat-treated composites (Table III). The variation of yield strength with reinforcement content (vol%) in the matrix is shown in Fig. 4.

The maximum increase in ultimate tensile strength with an increase in SiC reinforcement content from 20 vol% (312 MPa) to 30 vol% (352 MPa) is 13% for the as-extruded composite microstructure and nearly equal for the heat-treated counterpart. The variation of ultimate tensile strength as a function of heat treatment and reinforcement content is exemplified in Fig. 5.

Whereas the yield strength and ultimate tensile strength of the composite increase with an increase in particulate (SiC_p) reinforcement in the ductile aluminium alloy matrix, the ductility of the 2124 + SiC MMCs as measured by elongation over a 1 in. (2.54 cm) gauge length of the specimen decreases for both the as-extruded and heat-treated microstructures. The decrease in elongation with an increase in

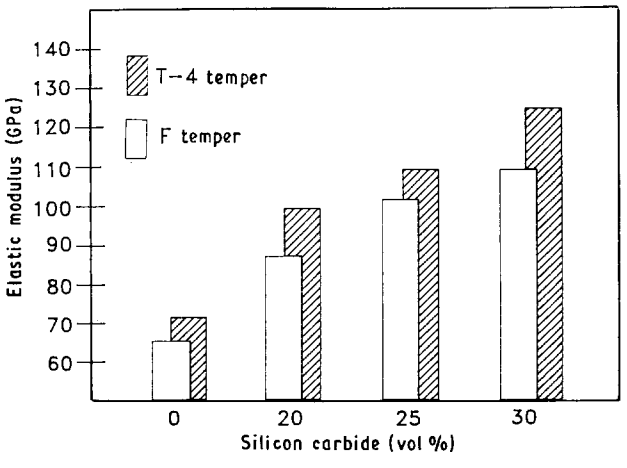

Figure 3 Variation of elastic modulus with reinforcement content.

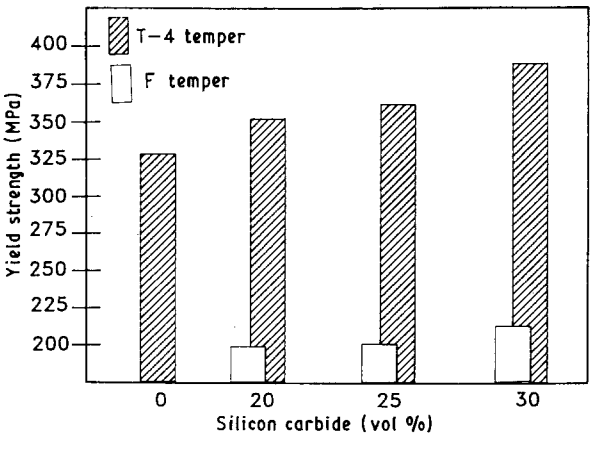

Figure 4 Variation of yield strength of the aluminium alloy composite with reinforcement content.

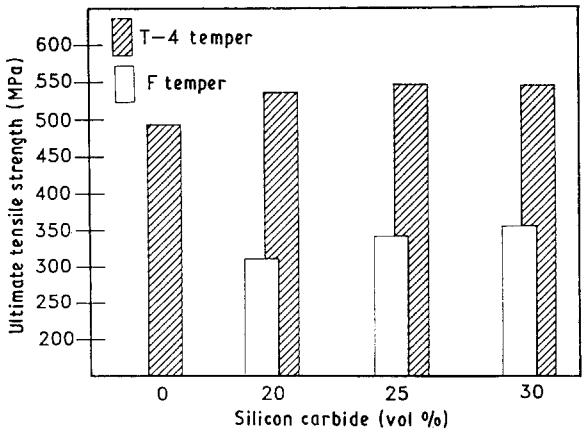

Figure 5 Variation of ultimate tensile strength of the aluminium alloy composite with reinforcement content.

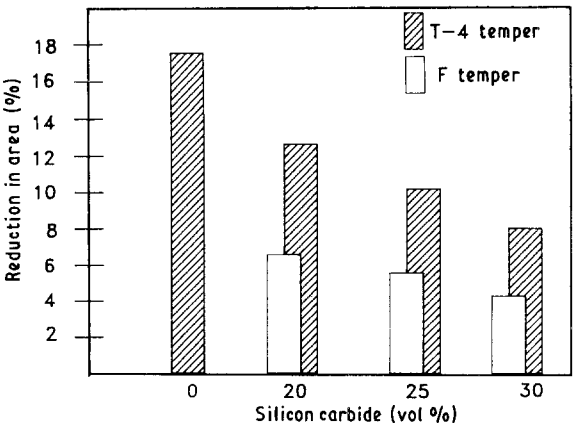

Figure 7 Influence of heat treatment and reinforcement content on reduction in area of the Al–SiC_p composite.

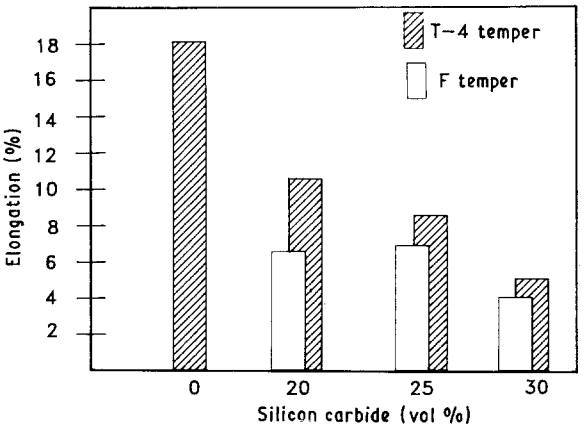

Figure 6 Influence of reinforcement content and heat treatment on tensile elongation of the Al–SiC_p composite.

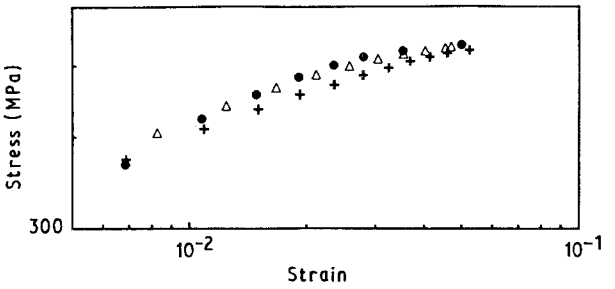

Figure 8 Monotonic stress–strain curves for the Al–SiC_p composite (+) 20 vol% SiC, (●) 25 vol% SiC, (△) 30 vol% SiC.

SiC_p content from 20 vol% to 30 vol% in the aluminium alloy matrix is:

(a) as high as 39% for the as-extruded composite microstructure, and

(b) as high as 51% for the heat-treated composite microstructure.

However, for a given volume fraction of SiC_p in the aluminium alloy matrix, heat treatment was found to improve the elongation of the MMC. The improvement in elongation was highest for the MMC with 20 vol% SiC_p reinforcement. The variation of elongation with reinforcement content and heat treatment is shown in Fig. 6. An increase in SiC reinforcement content caused a decrease in reduction in area for both the as-extruded and heat-treated composite microstructures. However, for a given volume fraction of reinforcement, the reduction in area of the composite significantly improved with heat treatment (Fig. 7).

Beyond macroscopic yield the stress–strain curve is well represented by a simple power law. It is expressed by the equation

$$\sigma = K(\varepsilon_p)^n \quad (1)$$

where K is the monotonic strength coefficient (intercept at $\varepsilon_p = 1$) and n is the strain-hardening exponent (slope). The monotonic strain hardening or work hardening exponent, n, of the Al/SiC_p composite decreases with an increase in reinforcement content. The value of strain-hardening exponent, n, of the MMCs is only marginally larger than the value of n for the matrix material with no reinforcement (0.13). The observed marginally higher strain-hardening exponent of the Al/SiC_p MMCs, in the heat-treated condition, as compared to that of the unreinforced matrix material, is attributed in part to particulate-induced changes in matrix triaxiality. The monotonic stress–strain curve for the three composites is shown in Fig. 8.

Several mechanisms of strengthening or hardening have been proposed which, either independently or concurrently, are considered responsible for the overall strength of the metal-matrix composite. The plausible mechanisms for this SiC particulate-reinforced 2124 aluminium alloy include:

(a) an overall strengthening resulting from strengths of the individual components of the composite as per the rule of mixtures theory [44];

(b) load transfer between the ductile aluminium alloy matrix and the hard and brittle carbide particle reinforcement [18, 44, 45];

(c) development of strengthening precipitates in the ductile aluminium alloy matrix during heat treatment resulting in the observed improvement in strength of the heat-treated composite over the as-extruded counterpart, for a given volume fraction of SiC reinforcement. In a comprehensive study of microstructural development in 2124 aluminium alloy reinforced with SiC whiskers, Christman and Suresh [22] observed

the strengthening S′ (Al_2CuMg) precipitates to nucleate on dislocations in the matrix of the composite. The extent of matrix precipitation was found to be significantly more than along the interfaces;

(d) enhanced dislocation density in the ductile aluminium alloy matrix due to the presence of the hard and brittle SiC particle [14, 16]. The increased dislocation density facilitates the nucleation of strengthening S′ precipitates in the matrix during heat treatment;

(e) strengthening arising from constrained plastic flow and triaxiality in the ductile aluminium alloy matrix due to the presence of brittle silicon carbide reinforcements [9, 11, 27]. As a result of the SiC particulates resisting plastic flow of the matrix, an average internal stress in the matrix or back stress, σ_b, is generated. The amount of back stress can be estimated by a dislocation-based model [46], or a continuum model [47, 48];

(f) contributions arising from competing influences of back stresses in the plastically deforming composite matrix [47] and due to plastic relaxation by the formation of prismatic dislocation loops around the hard particles [48];

(g) residual stresses generated in the matrix and plastic strains introduced near the reinforcement particles during cooling from the processing temperature as a result of mismatch in thermal expansion coefficients (CTE) between the components; the matrix and reinforcement [10, 49, 50];

(h) intrinsic differences in texture between the composite matrix and the matrix material without reinforcement [51].

In this metal-matrix composite (2124 + SiC_p) with large CTE mismatch strain, the plastic deformation of the ductile aluminium alloy matrix, in the presence of SiC reinforcement, is likely to be non-uniform. The plastic deformation-induced dislocations would become dominant when the plastic strain exceeds the thermal mismatch strain and the two effects would then act in synergism, so they can be lumped together. The strengthening, $\Delta\sigma$, in the metal matrix of this particulate-reinforced MMC, due to dislocation generation, can be estimated by

$$\Delta\sigma = \alpha G\boldsymbol{b}(\bar{\rho})^{1/2} \quad (2)$$

where α is a constant, G is the shear modulus (GPa) of the matrix metal, $\boldsymbol{b}$ is the Burgers vector of the matrix metal and $\bar{\rho}$ is the average density of dislocations generated in the matrix by CTE mismatch. The dislocation generation due to CTE mismatch in the two-phase material has been confirmed by several other investigators [52, 53]. Taya and Mori [54] showed that the punching of dislocations generated by CTE mismatch strain in a particulate-reinforced MMC is sufficiently extensive to cover most of the matrix domain. This observation was subsequently confirmed by transmission electron microscopy studies on aluminium alloy 2124 reinforced with SiC whiskers by Christman and Suresh [22]. The dislocations generated by the CTE mismatch strain can be at best be considered as an example of geometrically necessary dislocations defined by Ashby [46]. The increase in flow stress, $\Delta\sigma$, of the reinforced metal matrix over the unreinforced metal matrix is proportional to the square root of CTE mismatch strain if the dislocations generated by the CTE mismatch strain is dominant.

Based on results obtained in this study and an examination of the plausible strengthening mechanisms, we feel that major contributions to strength of the 2124 + SiC_p composite arise from the competing and synergistic influences of several of these mechanisms, the most important being:

(i) presence of strengthening S′ precipitates in the matrix,

(ii) strengthening due to mismatch in thermal coefficients of expansion, α_{CTE}, and

(iii) the back stress (σ_b).

4.3. Fracture behaviour

The monotonic fracture surfaces are helpful in elucidating microstructural effects on ductility and fracture properties of the metal-matrix composite. It is well established that the fracture of unreinforced alloys is associated with void nucleation and growth, with the nucleation occurring at the coarse constituent particles in the microstructure [55, 56]. An essential requirement for void nucleation is the development of a critical normal stress across the particle or the particle–matrix interface [57]. In the metal matrix with no reinforcement, nucleation of cavities occurs by:

(a) decohesion at an interface between the constituent particle and the matrix, and

(b) by cracking of the elastic inclusion.

Although the Al–SiC metal-matrix composites used in this study exhibited limited ductility on a macroscopic scale, with fracture essentially normal to the stress axis, examination of the fracture surface at high magnification revealed features reminiscent of a locally ductile mechanism. Few tear ridges were evident on the tensile fracture surfaces (Fig. 9). On a macroscopic scale the fracture surfaces were flat, but relatively rough when viewed on a microscale. The matrix of the composite was covered with a population of microvoids of a wide range of sizes (Fig. 10). The voids were homogeneously distributed throughout the fracture surface. The voids were intermingled with shallow dimples (Fig. 11). The constraints induced by the brittle SiC particles in the adjoining matrix and the resultant development of matrix triaxiality influences the flow stress of the composite, and also ductile void growth. Under the influence of far-field tensile loading the voids appear to have undergone limited growth confirming a possible contribution from particle constraint-induced triaxiality on failure of the composite matrix. Assuming that the particle–matrix interface is strong, the triaxial stresses generated during far-field tensile loading favours limited growth of microvoids in the matrix of the composite. The limited growth of voids during far-field tensile loading and lack of their coalescence as a

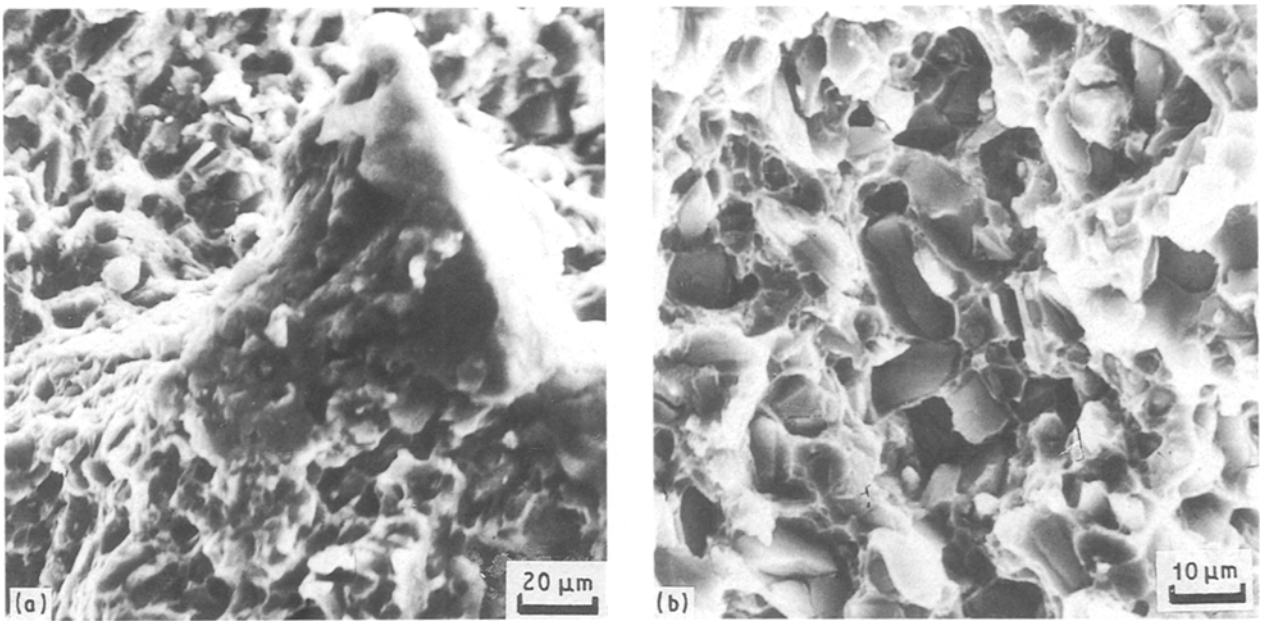

Figure 9 Scanning electron micrograph of the heat-treated tensile sample showing tear ridges and isolated patches of dimples: (a) 25 vol% SiC_p, (b) 30 vol% SiC_p.

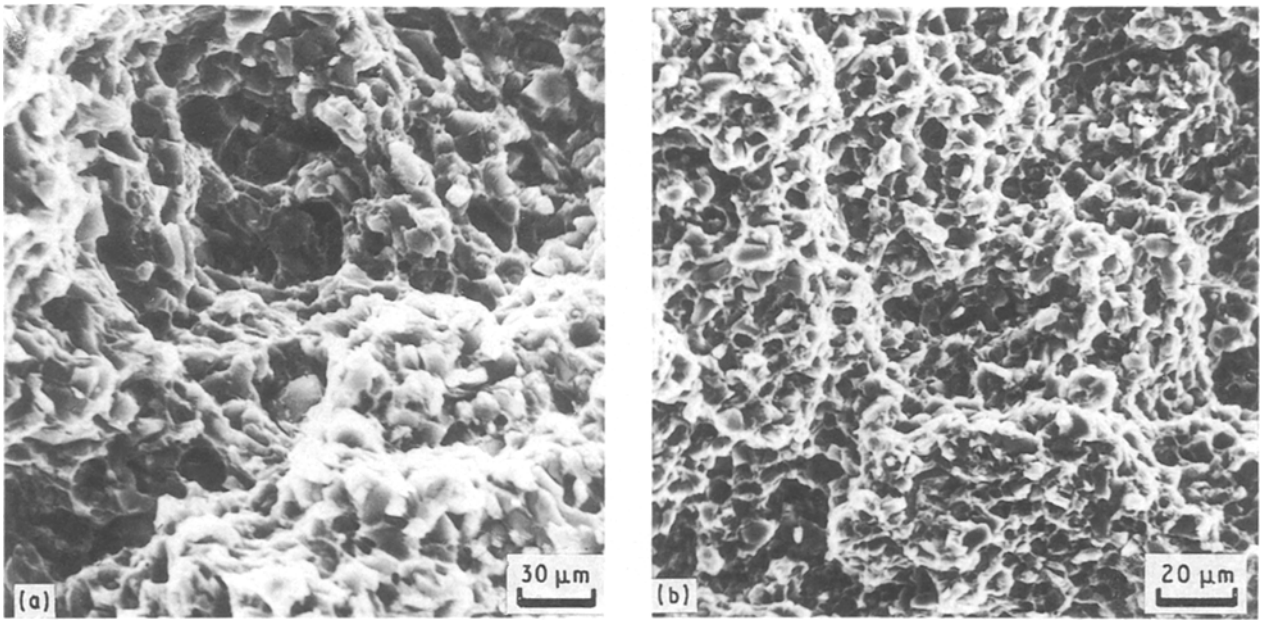

Figure 10 Scanning electron micrographs of the tensile sample showing microvoids of a range of sizes for the heat-treated composite: (a) 25 vol% SiC_p; (b) 30 vol% SiC_p.

fracture mode for this 2124Al–SiC_p composite clearly indicates that the deformation properties of the aluminium matrix are significantly altered by the SiC particles. The presence of these particles raises the hydrostatic component of stress, σ_T, and hence, their distribution is an important factor governing fracture of the composite.

For the as-extruded composite microstructure, the build-up of large stresses in the immediate vicinity of the reinforcing SiC particles coupled with mismatch that exists between the hard and brittle particle and the ductile aluminium alloy matrix, results in a large concentration of stress at and near the particle causing it to crack (Fig. 12a), and the matrix in the immediate vicinity to fail prematurely (Fig. 12b). Fracture of the brittle SiC particle and concurrent failure of the surrounding matrix results in the formation and presence of voids. Very few of the fine microvoids coalesce and the halves of these voids are the shallow dimples visible on the fracture surface (Fig. 9). With an increase in reinforcement content in the aluminium alloy matrix, fracture was found to be dominated by cracking of the SiC particles (Fig. 12b) on account of their intrinsic brittleness. The early cracking of the particles is largely responsible for the lower tensile ductilities of the as-extruded composites.

Intrinsic differences in the strain localization tendencies in the as-extruded and heat-treated composite microstructures also has an important influence on particle fracture. For a given volume fraction of re-

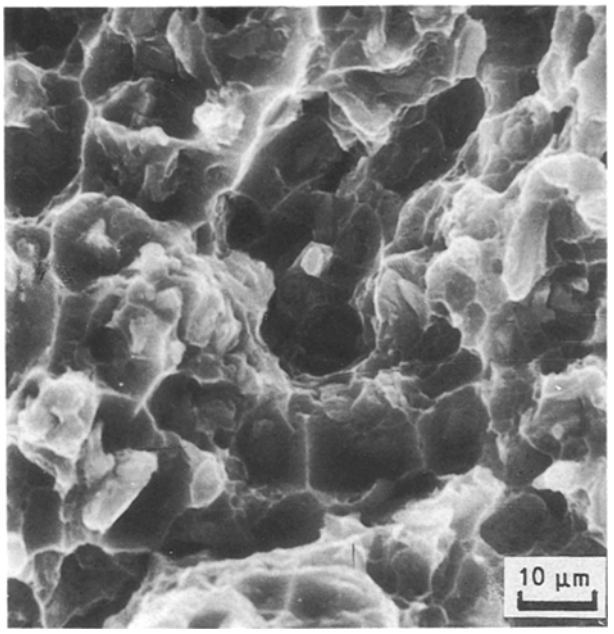

Figure 11 Scanning electron micrograph of tensile fracture surface of heat treated Al–SiC_p showing shallow dimples.

inforcement, in the aluminium alloy matrix, the density of fractured particles was found to be higher in the as-extruded composite microstructure than in the heat treated and aged temper. The overall "damage" resulting from uniaxial straining of this Al–SiC metal-matrix composite is due to the conjoint action of:

(a) damage associated with the reinforcement, such as SiC particle cracking and/or decohesion at the particle–matrix interface, and

(b) lattice damage such as dislocations and point defects, coupled with residual stress effects associated with the particles.

For the SiC particles to fracture they must be loaded to their fracture stress. This can be achieved, in principle, by shear loading through the interface. The extent of particle loading by the shear mechanism is dependent on the aspect ratio of the reinforcing particle. For symmetrically packed particles, the aspect ratio, S_s, for maximum loading is

$$S_s = \frac{\sigma_{SiC}}{\tau_i} \tag{3}$$

where σ_{SiC} is the strength of the particle and τ_i is the interfacial shear strength. The strength of monolithic SiC is about 2000 MPa, and assuming $\tau_i = \sigma_m/2$, where σ_m is the maximum stress achieved in the aluminium alloy matrix (about 550 MPa), the critical aspect ratio is 7. This shear mechanism approach ignores any end-loading effects, which would exert additional stress on the particle. Considering that during uniaxial tensile deformation a close observation of the fracture surface revealed less than 15%–20% of the SiC particles had fractured, either for the as-extruded or heat-treated composite microstructures, majority of the particles are, therefore, not loaded to their fracture stress. This situation is complicated by:

(i) the mismatch strain and concomitant internal stress in the composite due to differences in thermal expansion coefficient between the SiC particles and the aluminium alloy matrix. Assuming spherical shaped particles, the mismatch strain, α, will be induced in the particulates, and is equal to

$$\alpha = (\alpha_p - \alpha_M)\Delta T \tag{4}$$

where α_p and α_m are CTE of the particulate and matrix, respectively, and both the aluminium alloy matrix and the silicon carbide particulates (SiC_p) are assumed to be isotropic in CTE and stiffness. For particle fracture to occur the applied stress will have to overcome any residual stress present in the particle;

(ii) loading the particulates through the mismatch or misfit strain generated during plastic flow as a

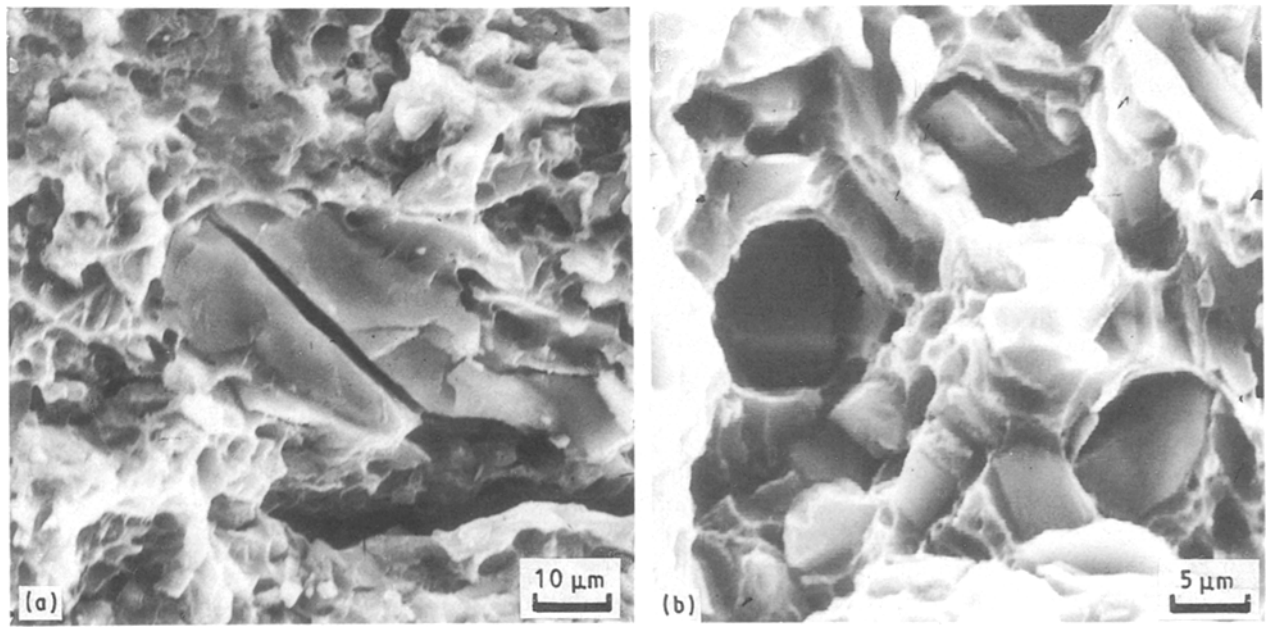

Figure 12 Scanning electron micrographs of the Al–SiC_p composite showing cracking at the reinforcement particle: (a) 20 vol% SiC_p; (b) 30 vol% SiC_p.

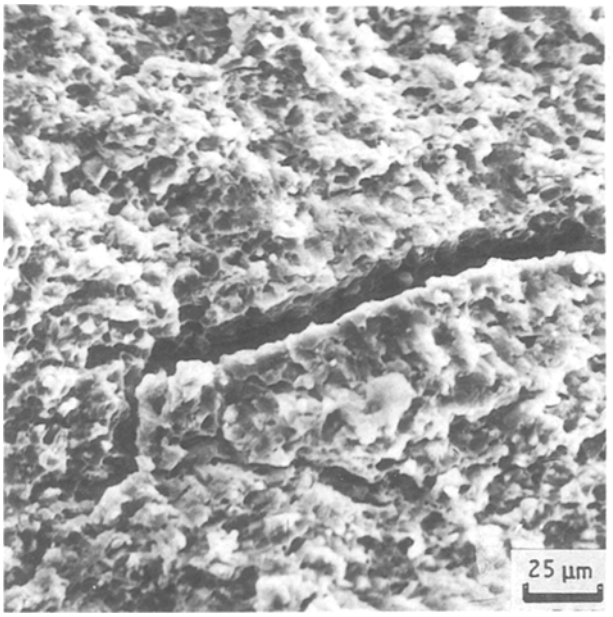

Figure 13 Scanning electron micrograph of the Al–SiC_p composite showing fracture through the matrix.

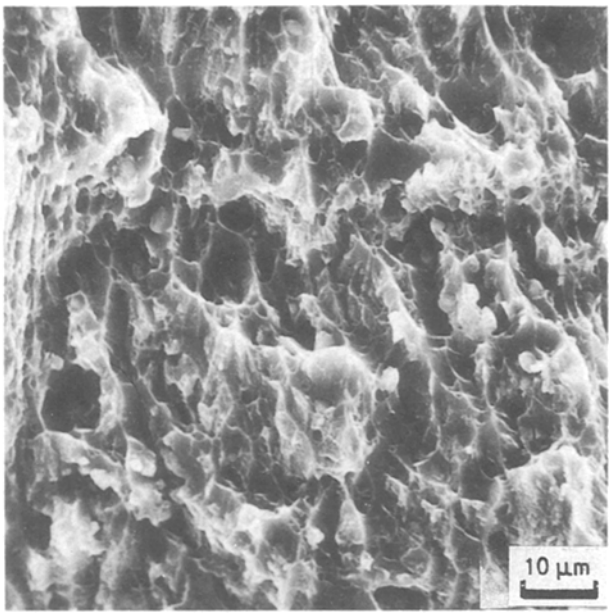

Figure 14 Scanning electron micrograph of tensile fracture surface of the unreinforced 2124 alloy.

result of the difference in elastic modulus between the hard particle and the soft matrix.

The stress, σ_r, at the interface of an elastic inclusion embedded in a plastic matrix was found to be tensile in nature, and is given by [57–59]

$$\sigma_{Tr} \simeq \sigma(\varepsilon_p) + \sigma_T \quad (5)$$

where $\sigma(\varepsilon_p)$ is the matrix yield stress at the plastic strain locally attained adjacent to the SiC particle, and σ_T is the tensile hydrostatic stress developed in the immediate vicinity or neighbourhood of the reinforcing particle. When the radial stresses generated at an interface exceed the SiC particle strength, particle cracking occurs. However, for SiC particle cracking to be important, a critical level of cracking is required before macroscopic tensile fracture results by crack growth through the ductile aluminium alloy matrix.

The essential difference in the tensile elongations between the unreinforced metal matrix (2124) and the reinforced metal matrices brings out:

(a) the presence of cracked particles in the composites, and

(b) the existence of higher triaxial tensile stresses in the composite matrix due to the presence of reinforcements.

For the reinforced metal matrix the majority of damage is associated with the particle clusters, and is in the form of voids which have grown between the particles or as cracked particles. The fracture initiates by particle cracking coupled with decohesion of the matrix between the particles, and final fracture is achieved by fracture through the matrix between the particle clusters (Fig. 13). The few voids generated by particle cracking did not grow extensively in the tensile direction, which is generally the case in ductile fracture of unreinforced alloys (Fig. 14) [60, 61]. The lack of extensive void growth in these high particulate volume fraction reinforced composites also suggests that the fracture strain is controlled by the void nucleation strain and any linkage strain.

5. Conclusion

Based on the results of this investigation on the influence of heat treatment on tensile properties and quasi-static fracture behaviour of discontinuous SiC–Al composites, for different volume fractions of SiC reinforcement, the following key observations were made.

1. The microstructure of the as-extruded composite showed the silicon carbide particulates to be dispersed randomly through the metal matrix with agglomeration of particulates at regular intervals. Heat treatment of the composite was found to have no influence on particulate size, distribution and agglomeration.
2. For a given condition, increasing the discontinuous SiC reinforcement increased both elastic modulus and strength of the metal-matrix composite.
3. The heat treated, i.e. aged, composite exhibited improved strength and ductility over the fabricated (as-extruded) counterpart.
4. Essentially, the increased strength of the discontinuous SiC–Al composite can be rationalized in terms of mechanisms based on a change in microstructure of the matrix due to the presence of the reinforcement. Presence and/or precipitation of matrix-strengthening precipitates during ageing, coupled with residual stresses generated due to intrinsic differences in thermal expansion coefficients between the components of the composite, and constrained plastic flow due to the presence of the reinforcement, contribute to the overall strengthening of the composite.
5. The non-uniform distribution of SiC particles caused fine microcracks to initiate at low stresses. The cracks initiated both at or near particle–matrix interfaces within clusters of particles. Fractography revealed an overall macroscopically brittle appearance,

but microscopically features were reminiscent of ductile rupture.

6. The tensile elongation is very sensitive to matrix microstructure. The low tensile ductility of the as-extruded composites is attributed to the early initiation of microcracks in the particle clusters due to elastic misfit coupled with plastic constraints imposed by the reinforcing particles. The matrix between the particles is subjected to high triaxial stress which results in fracture of the matrix between the particle clusters.

7. Fracture of the matrix between particle clusters, coupled with particle fracture, allows the microcrack to grow rapidly and link by fracture through the matrix resulting in macroscopic fracture.

Acknowledgements

This research was partially supported by ALCO Foundation (Grant No. 540341–843) and The University of Akron (Faculty Research Grant No. 1101). Material used in this study was provided by DWA Composite Specialties Inc., Chatsworth, CA (Program Manager Dr W. C. Harrigan Jr).

References

1. L. N. MUELLER, J. L. PROHASKA and J. W. DAVIS, in "Proceedings of AIAA Aerospace Engineering Conference" (AIAA, Los Angeles, CA, 1985).
2. C. R. CROWE and D. F. HASSON, in "Strength of Metals and Alloys: Proceedings of the Sixth International Conference", edited by R. C. Gifkins, ICSMA-6, Melbourne, Australia (Pergamon Press, London, 1982).
3. T. G. NEIH, *Metall. Trans.* **15A** (1984) 139.
4. D. L. McDANELS, *ibid.* **16A** (1985) 1105.
5. W. A. LOGSDON and PETER K. LIAW, *Engng Fract. Mech.* **24** (1986) 737
6. D. MOTT and PETER K. LIAW, *Metall. Trans.* **19A** (1988) 2233.
7. D. L. DAVIDSON, *ibid.* **18A** (1987) 2125.
8. S. MANOHARAN and J. J. LEWANDOWSKI, *Acta Metall.* **38** (1990) 489.
9. D. C. DRUCKER, in "High Strength Materials", edited by V. F. Zackey (Wiley Interscience, New York, 1965) pp 21–31.
10. D. A. KOSS and S. M. COPLEY *Metall. Trans.* **2A** (1971) 1557.
11. T. W. BUTLER and D. C. DRUCKER, *J. Appl. Mech.* **40** (1973) 780.
12. A. P. DIVECHA, C. R. CROWE and S. G. FISHMAN, 'Failure Modes in Composites IV" (Metallurgical Society of AIME, Warrendale, PA, 1977) 406.
13. A. P. DIVECHA, S. G. FISHMAN and S. D. KARMARKAR, *J. Metals* **33** (1981) 12.
14. R. J. ARSENAULT and R. M. FISHER, *Scripta Metall.* **17** (1983) 67.
15. T. G. NEIH and R. F. KARLAK, *J. Mater. Sci. Lett.* **2** (1983) 119.
16. R. J. ARSENAULT *Mater. Sci. Engng* **64** (1984) 171.
17. T. G. NEIH and D. J. CHELLMAN, *Scripta Metall.* **18** (1984) 925.
18. V. C. NARDONE and K. M. PREWO, *ibid.* **20** (1986) 43.
19. R. J. ARSENAULT and N. SHI, *Mater. Sci. Engng* **81** (1986) 175.
20. S. R. NUTT and A. NEEDLEMAN, *Scripta Metall.* **21** (1987) 705.
21. R. J. ARSENAULT and S. B. WU, *Mater. Sci. Engng* **96** (1987) 77.
22. T. CHRISTMAN and S. SURESH, *Acta Metall.* **6** (1988) 1691.
23. *Idem, Mater. Sci. Engng* **102A** (1988) 221.
24. H. J. RACK, *Adv. Mater. Manufact. Process.* **3** (1988) 327.
25. J. J. LEWANDOWSKI, C. LIU and WARREN H. HUNT Jr, in "Powder Metallurgy Composites", edited by P. Kumar, K. Vedula and Ann Ritter (Metallurgical Society of AIME, Warrendale, PA, 1989).
26. H. J. RACK, *idib.*
27. T. CHRISTMAN, A. NEEDLEMAN, S. R. NUTT and S. SURESH, *Mater. Sci. Engng* **107A** (1989) 49.
28. J. J. LEWANDOWSKI, C. LIU and WARREN H. HUNT Jr, *ibid.* **107A** (1989) 2412.
29. JIAN KU SHANG and R. O. RITCHIE, *Metall. Trans.* **20A** (1989) 897.
30. SHINJI KUMAI, J. E. KING and JOHN F. KNOTT, *Fat. Fract. Engng Mater. Struct.* **13** (1990) 511.
31. R. J. ARSENAULT, L. WANG and C. R. FENG, *Acta Metall.* **39** (1991) 47.
32. D. L. DAVIDSON, *Engng Fract. Mech.* **33** (1989) 965.
33. *Idem, Metall. Trans.* **22A** (1991) 97.
34. *Idem, ibid.* **22A** (1991) 113.
35. T. S. SRIVATSAN, RAHUL AURADKAR and AMIT PRAKASH *Engng Fract. Mech.* **40** (1991) 277.
36. T. S. SRIVATSAN, RAHUL AURADKAR, AMIT PRAKASH and E. J. LAVERNIA *Mater. Trans. Jpn Inst. Metals* July **32** (1991) 473.
37. T. S. SRIVATSAN and R. AURADKAR, *J. Mater. Sci. Lett.* **10** (1991) 500.
38. T. S. SRIVATSAN, R. AURADKAR and AMIT PRAKASH, in "Low Density High Strength Aluminium Alloys", edited by E. W. Lee (Metallurgical Society of AIME, Warrendale, PA, 1991) pp 385–404.
39. T. S. SRIVATSAN, I.A. IBRAHIM, E. J. LAVERNIA and F. A. MOHAMED, *J. Mater. Sci.* **26** (1991) 5965.
40. S. V. NAIR, J. K. TIEN and R. C. BATES, *Int. Metals Rev.* **30** (1985) 275.
41. C. MILLIERE and M. SUERY, *Mater. Sci. Technol.* **4** (1988) 41.
42. D. F. HASSON, C. R. CROWE, J. S. AHEARN and D. C. COOKE, "Failure Mechanisms in High Performance Materials (Cambridge University Press, Cambridge, 1985) p. 147.
43. D. L. DAVIDSON, *J. Mater. Sci.* **24** (1989) 965.
44. K. CHO and J. GURLAND, *Metall. Trans.* **19A** (1988) 2027.
45. V. C. NARDONE, *Scripta Metall.* **21** (1987) 1313.
46. M. F. ASHBY, *Philos. Mag.* **8** (1970) 399.
47. K. TANAKA and T. MORI, *Acta Metall.* **18** (1970) 931.
48. L. M. BROWN and W. M. STOBB, *Philos. Mag.* **23** (1971) 1185.
49. W. J. CLEGG, *Acta Metall.* **36** (1988) 2141.
50. M. TAYA, K. E. LULAY and D. J. LLOYD, *Acta Metall.* **39** (1991) 73.
51. R. J. ARSENAULT, L. WANG and C. R. FENG, *ibid.* **30** (1991) 47.
52. K. K. CHAWLA and M. METZGER, *J. Mater. Sci.* **7** (1972) 34.
53. M. VOGELSANG, R. J. ARSENAULT and R. M. FISHER, *Metall. Trans.* **17A** (1986) 379.
54. M. TAYA and T. MORI, *Acta Metall.* **35** (1987) 155.
55. F. A. McCLINTOCK, "Ductility" (American Society for Metals, Metals Park, Cleveland, OH, 1968) p. 256.
56. R. H. VAN STONE, T. B. COX, J. R. LOW Jr, and J. A. PSIODA: *Int. Metals Rev.* **30** (1985) 157.
57. A. S. ARGON, J. IM and R. SAFOGLU,*Metall. Trans.* **6A** (1975) 825.
58. J. ORR and D. K. BROWN, *Engng Fract. Mech.* **6** (1974) 261.
59. R. D. THOMPSON and J. W. HANCOCK, *Int. J. Fract. Mech.* **24** (1984) 209.
60. G. LE ROY, J. D. EMBURY, G. EDWARDS and M. F. ASHBY, *Acta Metall.* **29** (1981) 1509.
61. T. S. SRIVATSAN, D. LANNING Jr and K. SONI, *J. Mater. Sci.* in press.

Received 17 June
and accepted 16 December 1991